Beekman, Richard A.

1999

# Equilibrium configuration of systems of trapped ions

Department of Chemistry and Biochemistry

# Equilibrium configurations of systems of trapped ions

Richard A. Beekman and Marc R. Roussel
*Department of Chemistry, University of Lethbridge, Lethbridge, Alberta, Canada T1K 3M4*

P. J. Wilson*
*Department of Physics, University of Lethbridge, Lethbridge, Alberta, Canada T1K 3M4*

(Received 25 August 1998)

We have computed the equilibrium conformations of clusters of up to 100 ions in a spherically symmetric harmonic trap by a simple optimization strategy called seeding in which ions are added or removed from previously discovered minima. In each case, we have found at least as good a minimum as was previously known and believe that we have located the global minimum. We have additionally located a number of local minima and some saddle points. A balancing condition between the Coulomb and trapping terms which all of the critical points of the potential energy surface must satisfy was used to estimate the errors in the computed energies. [S1050-2947(99)09401-9]

PACS number(s): 02.60.Pn, 32.80.Pj, 52.25.Wz, 36.40.Mr

## I. INTRODUCTION

It is now possible to trap small numbers of ions at millikelvin temperatures in a harmonic trap and to observe their equilibrium configurations directly [1]. In two recent papers [2,3], the lowest-energy equilibrium configurations were computed. However, the energies of the configurations obtained were only reported to three or four decimal places, which is not always sufficient to distinguish equilibrium configurations one from another [4–6]. Furthermore, some interesting features of the equilibrium geometries of these systems were not discussed. We therefore recomputed the equilibrium geometries and energies of harmonically trapped ionic systems. In addition to searching for global energy minima, our method locates local minima and saddle points, an important first step in dynamical studies [7].

We seek the global minima of a set of $N$ ions interacting by the Coulomb force in a spherically symmetric harmonic potential. In dimensionless form, the potential is [8,9]

$$u=\sum_{i=1}^{N-1}\sum_{j=i+1}^{N}\frac{1}{r_{ij}}+\frac{1}{2}\sum_{i=1}^{N}r_i^2, \tag{1}$$

where $r_{ij}$ is the distance between ions $i$ and $j$, and $r_i^2=x_i^2+y_i^2+z_i^2$.

We report an efficient, reliable method for locating the global equilibrium and other critical points of this problem and, in general, of any particle cluster. Our method relies on the fact that the critical points corresponding to an $N$-particle cluster are generally closely structurally related to the $N+n$ and $N-n$ critical points for small values of $n$ [10]. Our strategy has allowed us to find lower-energy minima than had previously been reported for several values of $N$ and to discover local equilibria unreported in earlier studies. Along the way, we rediscovered the fact that the trapping and Coulomb terms of the potential have a simple relationship to each other at any equilibrium point [11]. We used this balancing condition to estimate the errors in our computed energies, as was originally suggested by Lozovik and Mandelshtam [11].

## II. COMPUTING METHODS

We initially intended to compute the global equilibria by simulated annealing [12], refining the crude solutions so obtained by simple downhill optimization. However, this approach proved to be both inefficient and unreliable. We therefore wrote a pair of programs which use simple, fast optimizers to perturb precomputed solutions by adding and removing particles. This strategy has been called ''seeding'' [13]. One optimizer uses a simple strategy similar to simulated annealing at zero temperature: Steps of a given size are taken along each of the coordinate axes in turn in the downhill direction until no further reduction in the energy can be achieved at this step size, at which point the step size is decreased and the process iterated until the step size has been reduced to a preselected threshold. The other optimizer is a simple gradient minimizer. Starting with large step sizes, the first optimizer is able to step out of shallow minima so that it is somewhat biased toward finding low-energy equilibria and is thus ideally suited to searching for the global minimum. The gradient optimizer was mostly used to refine previously discovered minima, as necessary, but was also found to be effective for finding higher-energy critical points.

A straightforwardly written optimizer must compute a very large number of square roots in cluster problems such as this, resulting in very poor performance. The simple downhill and simulated annealing strategies call for particles to be moved one at a time. If particle $k$ is moved, only the terms involving the coordinates of this particle in the energy [Eq. (1)] are affected. Our simple downhill and simulated annealing codes maintain a matrix of $1/r_{ij}$'s and a vector of trapping terms $r_i^2$. At every step, only those terms affected by the move are updated.

*Permanent address: Division of Science, Technology, Trades and Business, Medicine Hat College, Medicine Hat, Alberta, Canada T1A 3Y6.

 

TABLE I. Equilibrium configurations of ions in a spherically symmetric trap. $N$ is the number of ions, $u$ is the value of the potential energy at the equilibrium, $r_i$ is the distance of an ion from the origin, and $n_i$ is the number of ions at that distance. Up to $N=12$, the minimum energy configuration consists of a single shell. However, a second equilibrium with a central ion appears as early as $N=9$.

| $N$ | $u$ | $r_i(n_i)$ |
|---|---|---|
| 2 | 1.190 551 | 0.6300 (2) |
| 3 | 3.120 126 | 0.8327 (3) |
| 4 | 5.669 645 | 0.9721 (4) |
| 5 | 8.910 031 | 1.0808 (3), 1.1036 (2) |
| 6 | 12.639 073 | 1.1850 (6) |
| 7 | 17.024 321 | 1.2483 (2), 1.2832 (5) |
| 8 | 21.864 287 | 1.3498 (8) |
| 9 | 27.214 434 | 1.4145 (6), 1.4304 (3) |
| | 27.448 336 | 0.0000 (1), 1.5124 (8) |
| 10 | 33.057 547 | 1.4812 (8), 1.4978 (2) |
| | 33.232 075 | 0.0000 (1), 1.5664 (6), 1.5740 (3) |
| 11 | 39.404 080 | 1.5240 (1), 1.5404 (2), 1.5412 (2), 1.5436 (4), 1.5684 (2) |
| | 39.490 305 | 0.0000 (1), 1.6208 (8), 1.6296 (2) |
| 12 | 46.088 283 | 1.6001 (12) |
| | 46.234 432 | 0.0224 (1), 1.6667 (2), 1.6685 (1), 1.6695 (2), 1.6742 (4), 1.6877 (2) |

Our seeding programs allow random addition of an arbitrary number of particles as well as addition of a single particle to the center of the trap, random deletions, deletions of $n$ of the innermost particles or of $n$ of the outermost, as well as balanced deletions of an equal number of particles from the innermost and outermost positions of the cluster. (When an odd number of ions are to be removed, the balanced removal option removes one more ion from the outer shell than from the inner.) Seeding has previously been used in a limited way in cluster problems [3,13].

The seeding technique needs to be bootstrapped from a known solution. As we had simulated annealing solutions for many different values of $N$, we initially used these as seeds but could equally well have used the well-known analytic solutions of the problem for small $N$ [14,15]. Once we had a few minima for each value of $N$, these were in turn used as seeds for further trials. For smaller values of $N$, we used seeds differing by as many as ten ions from the desired configuration. For large values of $N$, additions or deletions of only one particle seemed to be sufficient to locate the global minima. Furthermore, for the largest clusters considered here, we focused our efforts on seeds which were within a few one-hundredths of an energy unit from the global minimum for their respective values of $N$. This still leaves hundreds of seeds from which to initiate the minimization process. Under these sampling restrictions, it becomes particularly important to use a combination of ordered and random additions/deletions to insure effective coverage of the configuration space.

The method described above, using either optimizer, has a tendency to locate both stable equilibria and saddle points, particularly for smaller values of $N$ [16]. This is particularly so when particles are being removed, due to the shell structure of the solutions [2,3,17,18]. If, for instance, we completely remove the inner shell, we are left with a configuration which is often in tangential equilibrium so that a critical point is easily accessible by a simple contraction of the outer shells. This critical point need not be a stable equilibrium. Accordingly, for all critical points located up to $N=47$ and for a selection of important points at higher $N$, we have computed the eigenvalues of the Hessian (the matrix of the second derivatives of $u$ with respect to the coordinates of the ions). A negative eigenvalue corresponds to an unstable direction in space. The index of a critical point is the number of negative eigenvalues [7]. A stable equilibrium point thus has an index of 0. Throughout this paper, we mostly focus our attention on stable equilibria, but discuss saddle points as appropriate [34].

One of the advantages of the seeding method is that the work can be distributed over several CPUs. Each optimizer run is relatively short and independent of the others. Accordingly, this method lends itself well to execution on several workstations coupled over a network. The workstations need not all be of the same design, nor need they be particularly fast. The computations described below were run on a mixture of Sun and Digital hardware of varying speeds.

## III. RESULTS AND DISCUSSION

Table I shows the energies and geometric characteristics of the minima of potential 1 for $N \leqslant 12$. For this range of values of $N$, the global minimum consists of a single, roughly spherical shell of ions. However, as has been previously noted [2,7], a second minimum appears on the potential energy surface at $N=9$ in which a shell of ions surrounds a single particle at the center of the trap. Note that the $(N-1,1)$ local minima appear not to have been previously reported for the 10- and 11-ion systems. A single shell of ions remains a local minimum on the potential energy surface for values of $N$ up to 23 (Table IV). For $N=24$, the single-shell critical point is a saddle point of index 5.

In one earlier study of this problem [14], it was errone-

TABLE II. Coulomb and harmonic trapping contributions to the energy for the unconstrained problem and for the case in which $r_1=r_2=\cdots=r_N$. Only the lowest-energy configuration is considered in these calculations. Note that the Coulomb energy is always exactly twice the trapping energy [11].

| | Unconstrained | | Constrained | |
|---|---|---|---|---|
| $N$ | Coulomb | Trapping | Coulomb | Trapping |
| 5 | 5.940 021 | 2.970 010 | 5.940 222 | 2.970 111 |
| 7 | 11.349 548 | 5.674 774 | 11.350 219 | 5.675 109 |
| 9 | 18.142 956 | 9.071 478 | 18.143 090 | 9.071 545 |
| 10 | 22.038 365 | 11.019 182 | 22.038 492 | 11.019 246 |
| 11 | 26.269 387 | 13.134 693 | 26.269 770 | 13.134 885 |

ously reported that the ions all lie at equal distances from the origin in the equilibrium conformation for $N=5$. It is easily verified by direct evaluation of the radial derivatives $\partial u/\partial r_i$ in this conformation that this is not the case. However, if we minimize the energy subject to the constraint that all of the ions are equidistant from the origin, we find that the energy is only slightly higher. For instance, for $N=5$, the energy of the constrained system is 8.910 334 with a radius equal to the average radius of the unconstrained system. Note that the constraint raises the energy by only $3\times10^{-4}$ dimensionless energy units, highlighting the importance of displaying energies to several decimal places when characterizing clusters.

The fact that ions trapped in a soft spherically symmetric potential do not in general have equilibrium positions lying on the surface of a sphere should come as no surprise for two reasons: First, it has been noted that in the Thomson problem, the electrostatic potential energy is not generally evenly distributed over all ions [19]. For instance, for $N=5$, the axial ions each contribute 1.2% more than the average to the total potential energy while the equatorial ions each contribute 0.8% less. Thus the Coulomb (ion-ion repulsion) contribution to the energy can be reduced by stretching the polar axis which, however, slightly increases the value of the corresponding trapping terms in potential 1. This allows a shortening of the radial distances in the equatorial plane which also reduces the trapping contribution to the potential energy. The results of constrained and unconstrained simulated annealing optimizations shown in Table II for small values of $N$ where asphericity occurs confirm our reasoning. In addition, we might have expected unequal radial distances by a rather simple argument: While the trapping potential is spherically symmetric, placing ions in the trap breaks this symmetry. It then becomes a question of whether the ions can be so positioned that they are all symmetry-equivalent. For some values of $N$ such as 5, 7, 9, 10, and 11, this is impossible [20] and unequal radial distances are to be expected. This effect is well known in structural chemistry, where the VSEPR method for predicting molecular geometries leads to an energy minimization problem of similar form for these values of $N$ [21].

We may also note from Table II that the Coulomb contribution to the energy is always exactly twice the contribution from the harmonic trapping terms of Eq. (1). This property has previously been noted [11] and follows from a simple scaling argument. Since this result is exact, it provides a useful check on the numerical accuracy of the minimization method used [11].

Transition states are saddle points of index 1, i.e., having one unstable direction [7]. Table III shows the transition states found during our search for minima for values of $N$ between 10 and 22. For $N<10$, the transition states are available from the paper of Wales and Lee [7] who used an eigenvector-following method to locate both minima and saddle points. Although the range $N=10$–$22$ was also studied by Wales and Lee, we have found several previously unreported transition states. Our method also missed some transition states which they detected. This suggests that a combination of seeded minimization and eigenvector following might be valuable to locate transition states of clusters for small values of $N$. Note that in a few cases noted in Table III, we located transition states of lower energy than previously reported. Clearly, these transition states may be of dynamical significance. We have also found a number of high-index saddle points and, of course, we have detected some transition states and other saddle points for higher values of $N$ (data not shown).

Tables IV, V, and VI show the minima located for various values of $N>12$. Due to the rapidly growing number of equilibria, we report progressively less information as $N$ increases. In several cases, we have found deeper minima than those reported by earlier workers. These new results are marked in the tables. Note that for $N=24$, while Rafac *et al.* [2] missed the global minimum, the correct configuration was located by Hasse and Avilov [3]. Also note that the inner-shell radius given for $N=27$ in Table II of Ref. [2] is much too large.

When reporting cluster structures and energies, it is important to show as many significant figures as can be reliably obtained because the minima are sometimes extremely closely spaced, as has previously been pointed out for the Thomson problem [5]. Consider, for instance, the third and fourth minima at $N=44$ (Table V) where we reported nine digits instead of six because of a difference of only $5.58\times10^{-7}$ units in their energies. Commonly used procedures for reporting energies of clusters, such as normalizing by the number of particles [3,22], especially when combined with a truncation of the energies after the third or fourth digit, sometimes make it difficult to establish whether a given critical point is or is not the same as another, especially when no geometric information (shell radii, point groups, etc.) is given.

Rafac *et al.* [2] found that the global minimum configuration for $N=60$ is a (48,12) configuration and wrote that a three-shell global minimum first appeared at $N=61$. However, this is not the first three-shell global minimum, as can

TABLE III. Transition states located for $N=10$–22. $N$ and $u$ have the same meanings as in Table I. The shell structure $(n_1,n_2,\ldots)$ of each transition state is given, where $n_1$ is the number of ions in the outer shell, $n_2$ is the number in the next shell, and so on.

| $N$ | $u$ $(n_1,n_2,\ldots)$ |
|---|---|
| 10 | 33.060 405 (10); 33.233 098 (9,1) |
| 11 | 39.405 154 (11); 39.492 811 (10,1) |
| 12 [a] | 46.169 678 (12); 46.182 042 (12); 46.198 479 (12); 46.235 417 (11,1) |
| 13 [a] | 53.364 232 (13); 53.387 302 (12,1); 53.398 774 (12,1) |
| 14 [a] | 60.958 829 (13,1); 61.010 378 (14) |
| 15 | 68.969 935 (14,1); 69.066 250 (15); 69.066 517 (15); 69.150 711 (15) |
| 16 [b] | 77.382 574 (15,1); 77.382 688 (15,1); 77.537 561 (16); 77.541 454 (16); 77.578 621 (16) |
| 17 [b] | 86.202 038 (16,1); 86.205 356 (16,1); 86.415 118 (17) |
| 18 | 95.419 407 (17,1); 95.686 963 (18); 95.762 664 (18) |
| 19 | 105.024 469 (18,1); 105.097 140 (18,1); 105.381 468 (19); 105.382 265 (19) |
| 20 | 115.044 405 (19,1); 115.109 600 (18,2); 115.111 184 (18,2); 115.165 817 (18,2); 115.396 809 (20) |
| 21 | 125.381 638 (20,1); 125.463 702 (19,2); 125.464 079 (19,2); 125.819 743 (21); 125.819 872 (21); 125.837 963 (21) |
| 22 [a,b] | 136.119 895 (21,2); 136.119 991 (21,1); 136.136 927 (20,2); 136.137 588 (21,1); 136.138 585 (20,2); 136.608 119 (22); 136.613 265 (22) |

[a]Wales and Lee [7] report additional transition states for values of $N$ so marked.
[b]The first configuration given is lower in energy than the lowest-energy transition state found by Wales and Lee [7].

be seen in Table VI. In the range $N=58$–61, with the exception of $N=60$, the global minimum is an $(N-13,12,1)$ configuration. The structure of the global minimum at $N=60$ is anomalous, belonging to the same genus as the global minima obtained for $N=55$–57. To understand this anomaly, we computed the specific excess energy [23],

$$u_e=\frac{u}{N}-\frac{9}{10}N^{2/3},$$

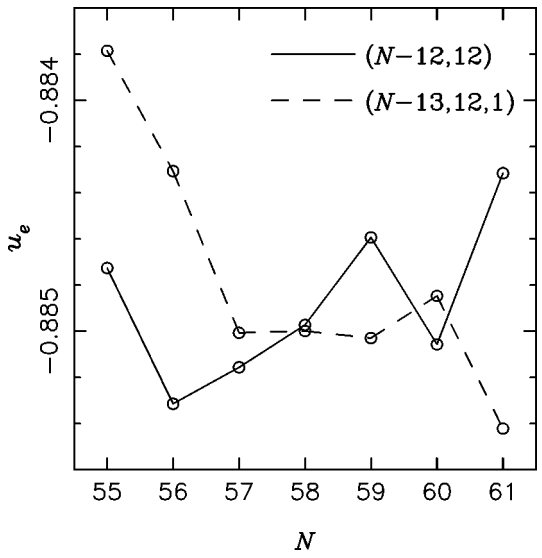


FIG. 1. Specific excess energies of the lowest-energy $(N-12,12)$ and $(N-13,12,1)$ clusters for $N=55$–61. Note that the $N=60(48,12)$ cluster is significantly more stable and that the (47,12,1) cluster is significantly less stable than the corresponding clusters for neighboring values of $N$.

the difference between the energy per ion and the energy of a homogeneous $N$-ion plasma. The results are shown for the lowest-energy $(N-12,12)$ and $(N-13,12,1)$ clusters for $N$ between 55 and 61 (Fig. 1). The $N=60$ clusters are anomalous in two ways: First, the (48,12) cluster is significantly more stable than the neighboring (47,12) and (49,12) clusters. Second, the (47,12,1) cluster is significantly less stable than its neighbors. The importance of the former fact has previously been emphasized [23]. However, the (48,12) cluster might not be a global minimum for $N=60$ if the (47,12,1) cluster were not somewhat higher in energy than might be expected from the excess energies of its neighbors. In a sense then it is not just the special stability or ''magic number'' property of $N=60$ which is responsible for the anomalous shell structure obtained at this value of $N$, but also an ''antimagic'' property which results in a less stable than expected three-shell configuration.

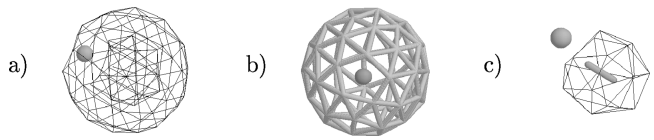


FIG. 2. Equilibrium configuration with an intershell ion for $N=79$ with an energy of 1239.116 475 units. Drawing (a) shows the whole cluster, with bonds represented by lines. The sphere is the intershell ion. The outer-shell ions lie between 3.46 and 3.68 units from the center of the trap. The ions in the next shell lie between 1.95 and 2.23 units from the center. The intershell ion is at a distance of 2.59 units from the center, belonging clearly neither to one shell nor to the other. Drawing (b) shows only the outer shell and the intershell ion. Note that this ion sits under a pentagonal hole in the outer shell. Drawing (c) shows only the intershell ion and the inner shells. The intershell ion almost lies along the ''bond axis'' of a two-ion innermost shell (drawn as a solid stick for emphasis).

TABLE IV. Equilibrium configurations for $N=13$–27. $N$ and $u$ have the same meanings as in Table I. However, in this case, only the shell average radius ($\overline{r_i}$) is given rather than the individual distances, the latter list being extremely long for some low-symmetry configurations.

| $N$ | $u$ | $\overline{r_i}(n_i)$ |
|---|---|---|
| 13 | 53.311 577 | 0.0000 (1), 1.7210 (12) |
| | 53.363 799 | 1.6542 (13) |
| 14 | 60.958 435 | 0.0089 (1), 1.7680 (13) |
| | 60.997 336 | 1.7043 (14) |
| 15 | 68.957 823 | 0.0000 (1), 1.8121 (14) |
| | 69.065 338 | 1.7520 (15) |
| 16 | 77.381 627 | 0.0000 (1), 1.8445 (15) |
| | 77.536 558 | 1.7974 (16) |
| | 77.542 086 | 1.7975 (16) |
| 17 | 86.200 931 | 0.0000 (1), 1.8951 (16) |
| | 86.205 854 | 0.0000 (1), 1.8952 (16) |
| | 86.413 661 | 1.8409 (17) |
| 18 | 95.417 840 | 0.0000 (1), 1.9344 (17) |
| | 95.683 733 | 1.8825 (18) |
| 19 | 105.021 479 | 0.0000 (1), 1.9722 (18) |
| | 105.378 552 | 1.9228 (19) |
| 20 | 115.041 825 | 0.0002 (1), 2.0091 (19) |
| | 115.109 516 | 0.6803 (2), 2.0518 (18) |
| | 115.396 053 | 1.9612 (20) |
| 21 | 125.380 818 | 0.0000 (1), 2.0443 (20) |
| | 125.458 622 | 0.6807 (2), 2.0861 (19) |
| | 125.819 715 | 1.9984 (21) |
| 22 | 136.119 890 | 0.0009 (1), 2.0788 (21) |
| | 136.136 927 | 0.6704 (2), 2.1193 (20) |
| | 136.138 274 | 0.6728 (2), 2.1192 (20) |
| | 136.603 134 | 2.0344 (22) |
| 23 | 147.201 472 | 0.6680 (2), 2.1516 (21) |
| | 147.201 540 | 0.6681 (2), 2.1515 (21) |
| | 147.213 301 | 0.0000 (1), 2.1121 (22) |
| | 147.222 935 | 0.0000 (1), 2.1122 (22) |
| | 147.284 451 | 0.8987 (3), 2.1877 (20) |
| | 147.789 663 | 2.0688 (23) |
| 24 | 158.615 707 [a] | 0.6627 (2), 2.1830 (22) |
| | 158.623 646 | 0.6631 (2), 2.1830 (22) |
| | 158.688 346 | 0.8872 (3), 2.2186 (21) |
| | 158.705 886 | 0.0000 (1), 2.1448 (23) |
| | 158.781 360 | 1.0435 (4), 2.2524 (20) |
| 25 | 170.414 660 | 0.6630 (2), 2.2137 (23) |
| | 170.425 714 | 0.8767 (3), 2.2488 (22) |
| | 170.490 241 | 0.0000 (1), 2.1762 (24) |
| | 170.530 042 | 1.0313 (4), 2.2823 (21) |
| 26 | 182.511 548 | 0.6604 (2), 2.2433 (24) |
| | 182.546 368 | 0.8732 (3), 2.2781 (23) |
| | 182.546 862 | 0.8737 (3), 2.2780 (23) |
| | 182.592 651 | 1.0179 (4), 2.3112 (22) |
| | 182.684 887 | 0.0006 (1), 2.2071 (25) |
| 27 | 194.955 099 | 0.8691 (3), 2.3063 (24) |
| | 194.956 830 | 0.8687 (3), 2.3063 (24) |
| | 195.008 599 | 0.6580 (2), 2.2726 (25) |
| | 195.008 884 | 0.6582 (2), 2.2726 (25) |
| | 195.025 549 | 1.0166 (4), 2.3390 (23) |
| | 195.031 087 | 1.0161 (4), 2.3389 (23) |
| | 195.197 517 | 0.0004 (1), 2.2371 (26) |

[a]Improves on the minimum found by Rafac *et al.* [2].

The shell structure of the solutions has frequently been emphasized, both in the spherically symmetric case [2,3,17,18] and in other geometries [24–28]. We find that while the vast majority of equilibrium configurations are made up of thin, distinct (''onion'' [3]) shells, there are cases in which intershell ions appear for larger values of $N$. Figure 2 shows such a case. The innermost shell consists of two ions located 0.57 and 0.85 units from the center of the trap. The 58-ion outermost shell contains a pentagonal hole. (A similar structure has previously been described in a much larger cluster by Hasse and Avilov [3].) This allows one of the ions which would have completed the middle shell to move out between the two shells, part way into the pentagonal hole in the outer shell. This leaves a pentagonal hole in the middle shell. The two-ion inner shell then aligns with this hole to minimize repulsions between it and the nearby middle-shell ions. (The intershell ion lies just 0.39 distance units off the line defined by the two inner-shell ions.) Similar pentagonal defects account for other intershell ion structures detected. The existence of such equilibrium structures opens the possibility that they exist as true intermediates on the reaction path between configurations whose two outer shells differ by the transfer of a single ion (and the attendant shell reorganizations). In the $N=79$ case, for instance, there are many (59,18,2) and (58,19,2) equilibria. One pair of these equilibria may be connected to each other through a reaction path that includes the structure shown in Fig. 2.

## IV. CONCLUSIONS

Previous computational studies of this system for small to moderate values of $N$ used molecular-dynamics simulations to obtain the minima by slow cooling. Despite precautions taken in these studies to avoid trapping in local minima, we have improved on several previously reported results as shown in Tables IV, V, and VI. We attribute our success to using a direct minimization method rather than a dynamical simulation. (Schweigert and Peeters have also found direct minimization of the potential energy to be an advantageous strategy [29].) While our minimization methods are simple, they have the virtue of having been specifically designed for this class of problems and are thus likely to outperform any dynamical method when the goal of the study is the location of the minima of a potential energy surface.

While we cannot be completely sure that we have found the global minimum in all cases, we are reasonably confident that we have in fact done so for all value of $N$ up to 100. We also believe that we have found all local equilibria up to $N=27$ and most of the equilibria up to $N=45$. As can be seen from Table V, the number of equilibria grows rapidly for $N$ between 28 and 45. The growth is even more spectacular beyond this point. Furthermore, the potential existence of multiple geometrically similar equilibria within a small fraction of an energy unit of each other makes an enumeration very difficult at larger values of $N$.

The balancing condition between Coulomb and trapping terms is of course specific to this problem, but similar relations hold for the equilibria of any potential where the energy depends on the distances between the particles in a simple way. For the Lennard-Jones potential, for instance, we find that the sum of the $r^{-6}$ terms of the potential is six

TABLE V. Equilibrium configurations for $N=28-45$. Due to the large number of minima, only the energies ($u$) and shell configurations are given, using the notation of Table III.

| $N$ | $u\ (n_1,n_2,\ldots)$ |
|---|---|
| 28 [a] | 207.754 525 (25,3); 207.754 861 (25,3); 207.754 883 (25,3); 207.757 587 (24,4); 207.761 305 (24,4); 207.820 597 (26,2); 207.820 639 (26,2); 207.821 200 (26,2); 208.021 508 (27,1) |
| 29 [a] | 220.861 155 (25,4); 220.868 858 (26,3); 220.868 889 (26,3); 220.869 561 (26,3); 220.869 913 (26,3); 220.940 151 (27,2); 220.943 692 (27,2); 221.227 874 (28,1) |
| 30 [a] | 234.275 743 (26,4); 234.290 674 (27,3); 234.291 012 (27,3); 234.437 023 (28,2); 234.437 223 (24,6) |
| 31 [a] | 248.003 508 (27,4); 248.003 667 (27,4); 248.004 973 (27,4); 248.006 531 (27,4); 248.078 950 (28,3); 248.080 272 (28,3); 248.095 601 (26,5); 248.102 062 (26,5); 248.106 719 (26,5); 248.183 469 (25,6); 248.183 650 (25,6); 248.274 570 (29,2) |
| 32 | 262.078 106 (28,4); 262.087 298 (28,4); 262.127 525 (27,5); 262.127 570 (27,5); 262.130 637 (27,5); 262.133 184 (27,5); 262.201 739 (29,3); 262.204 598 (29,3); 262.217 110 (26,6); 262.218 923 (26,6); 262.219 120 (26,6); 262.400 669 (30,2) |
| 33 | 276.499 367 (29,4); 276.500 868 (29,4); 276.507 922 (28,5); 276.509 007 (28,5); 276.509 450 (28,5); 276.550 448 (27,6); 276.616 322 (30,3); 276.863 432 (31,2) |
| 34 | 291.199 695 (30,4); 291.217 151 (29,5); 291.217 580 (29,5); 291.217 706 (29,5); 291.217 765 (29,5); 291.217 790 (29,5); 291.217 819 (29,5); 291.223 997 (28,6); 291.224 429 (28,6); 291.365 251 (31,3); 291.365 345 (31,3); 291.366 805 (31,3); 291.597 481 (32,2); 291.597 488 (32,2) |
| 35 | 306.206 160 (30,5); 306.206 924 (30,5); 306.206 976 (30,5); 306.207 512 (30,5); 306.209 295 (30,5); 306.223 414 (29,6); 306.224 242 (29,6); 306.224 286 (29,6); 306.230 346 (31,4); 306.230 740 (31,4); 306.232 137 (31,4); 306.381 724 (32,3); 306.381 784 (32,3); 306.458 660 (32,3); |
| 36 [b] | 321.503 649 (30,6); 321.504 163 (30,6); 321.517 753 (31,5); 321.519 925 (31,5); 321.521 600 (31,5); 321.524 426 (31,5); 321.529 463 (32,4); 321.607 914 (32,4); 321.622 095 (29,7); 321.624 774 (29,7); |
| 37 | 337.095 444 (31,6); 337.100 109 (31,6); 337.105 565 (32,5); 337.175 408 (32,5); 337.181 822 (32,5); 337.198 406 (30,7); 337.199 087 (30,7); 337.203 217 (30,7); 337.241 211 (33,4); |
| 38 [b] | 352.968 275 (32,6); 352.968 574 (32,6); 353.034 374 (32,6); 353.082 188 (31,7); 353.084 913 (31,7); 353.092 941 (33,5); 353.092 944 (33,5); 353.093 915 (33,5); 353.094 586 (33,5); 353.094 838 (33,5); 353.179 599 (30,8); 353.186 865 (30,8); 353.201 771 (34,4) |
| 39 | 369.233 127 (33,6); 369.233 144 (33,6); 369.243 764 (32,7); 369.245 082 (32,7); 369.295 859 (32,7); 369.306 533 (32,7); 369.306 778 (32,7); 369.328 732 (34,5); 369.331 774 (34,5); 369.333 422 (34,5); 369.481 043 (35,4); 369.481 079 (35,4); 369.485 427 (35,4); |
| 40 | 385.743 627 (34,6); 385.779 929 (33,7); 385.781 416 (33,7); 385.782 895 (33,7); 385.802 767 (32,8); 385.802 778 (32,8); 385.854 188 (32,8); 385.854 755 (32,8); 385.877 024 (35,5); 385.877 825 (35,5); 385.883 088 (35,5); 385.883 140 (35,5); 385.883 272 (35,5); 385.883 323 (35,5); 386.048 487 (36,4); 386.049 431 (36,4) |
| 41 [b] | 402.566 851 (35,6); 402.567 137 (36,5); 402.572 104 (34,7); 402.574 367 (34,7); 402.575 052 (34,7); 402.575 500 (34,7); 402.611 757 (33,8); 402.615 333 (33,8); 402.669 798 (32,9); 402.674 304 (32,9); 402.714 650 (36,5); 402.716 997 (36,5); 402.718 565 (36,5); 402.718 706 (36,5); 402.718 727 (36,5); 402.719 863 (36,5); 402.720 043 (36,5) |
| 42 | 419.664 273 (35,7); 419.665 253 (35,7); 419.669 185 (36,6); 419.669 521 (35,7); 419.669 953 (35,7); 419.670 399 (35,7); 419.678 983 (34,8); 419.679 356 (34,8); 419.683 912 (34,8); 419.686 368 (34,8); 419.763 024 (33,9); 419.853 743 (37,5); 419.854 754 (37,5); 419.857 658 (37,5); 419.857 922 (37,5); 419.859 587 (37,5); 419.861 496 (37,5) |
| 43 | 437.042 023 (36,7); 437.045 286 (36,7); 437.045 613 (35,8); 437.045 955 (36,7); 437.046 165 (36,7); 437.047 679 (35,8); 437.049 293 (36,7); 437.051 187 (35,8); 437.052 473 (35,8); 437.077 234 (37,6); 437.081 275 (37,6); 437.083 099 (36,7); 437.104 318 (34,9); 437.104 538 (34,9); 437.106 233 (34,9); 437.143 718 (36,7); 437.286 211 (38,5); 437.287 004 (38,5); 437.289 299 (38,5); 437.289 921 (38,5) |
| 44 [a] | 454.697 878 (36,8); 454.698 526 (36,8); 454.698 900 639 (36,8); 454.698 901 197 (36,8); 454.699 248 (36,8); 454.701 426 (36,8); 454.701 487 (37,7); 454.701 872 (36,8); 454.717 146 (37,7); 454.720 197 (37,7); 454.725 415 (37,7); 454.725 662 (37,7); 454.743 572 (35,9); 454.744 382 (35,9); 454.745 007 (36,8); 454.748 152 (35,9); 454.750 096 (35,9); 454.750 158 (35,9); 454.750 721 (35,9); 454.751 089 (35,9); 454.752 438 (35,9); 454.754 419 (35,9); 454.775 720 (38,6); 454.776 572 (38,6); 454.777 316 (38,6); 454.779 487 (38,6) |
| 45 [a] | 472.633 229 (37,8); 472.639 443 (37,8); 472.639 579 (37,8); 472.644 440 (37,8); 472.664 024 (36,9); 472.665 498 (36,9); 472.666 286 (36,9); 472.668 496 (36,9); 472.681 609 (38,7); 472.682 083 (38,7); 472.682 292 (38,7); 472.683 893 (38,7); 472.684 269 (38,7); 472.684 735 (38,7); 472.687 210 (38,7); 472.687 304 (38,7); 472.688 114 (38,7); 472.688 156 (38,7); 472.699 222 (36,9); 472.760 851 (39,6); 472.762 943 (39,6); 472.778 299 (39,6); 472.778 505 (39,6); 472.779 429 (39,6) |

[a]Lowest-energy equilibrium improves on the minimum found by Hasse and Avilov [3].

[b]Global minimum not found by simulated annealing.

TABLE VI. Global equilibrium configurations for large $N$. Due to the large number of minima, only the global minimum energy ($u$) is given, along with the average shell radii ($\overline{r}_i$) and occupation numbers ($n_i$) for the corresponding minimum.

| $N$ | $u$ | $\overline{r}_i(n_i)$ |
|---|---|---|
| 46 | 490.865 413 | 1.3660 (8), 2.8664 (38) |
| 47 | 509.364 892 | 1.4352 (9), 2.9062 (38) |
| 48 | 528.138 313 | 1.4337 (9), 2.9243 (39) |
| 49 | 547.197 840 | 1.4327 (9), 2.9421 (40) |
| 50 [a] | 566.532 661 | 1.4328 (9), 2.9596 (41) |
| 51 | 586.136 053 | 1.4964 (10), 2.9970 (41) |
| 52 | 606.011 001 | 1.4962 (10), 3.0140 (42) |
| 53 | 626.166 254 | 1.4958 (10), 3.0307 (43) |
| 54 [b] | 646.570 635 | 1.4958 (10), 3.0473 (44) |
| 55 | 667.231 207 | 1.6093 (12), 3.1017 (43) |
| 56 | 688.138 425 | 1.6089 (12), 3.1174 (44) |
| 57 | 709.348 383 | 1.6080 (12), 3.1333 (45) |
| 58 [a] | 730.818 457 | 0.0066 (1), 1.7343 (12), 3.1657 (45) |
| 59 [a] | 752.536 120 | 0.0000 (1), 1.7342 (12), 3.1809 (46) |
| 60 [a] | 774.510 781 | 1.6070 (12), 3.1795 (48) |
| 61 | 796.720 223 | 0.0052 (1), 1.7325 (12), 3.2112 (48) |
| 62 [b,c] | 819.214 999 | 0.0205 (1), 1.7808 (13), 3.2428 (48) |
| 63 [b,c] | 841.937 455 | 0.0059 (1), 1.8235 (14), 3.2743 (48) |
| 64 [b,c] | 864.932 364 | 0.0024 (1), 1.8241 (14), 3.2886 (49) |
| 65 [b] | 888.149 659 | 0.0000 (1), 1.8239 (14), 3.3025 (50) |
| 66 [a] | 911.637 142 | 0.0075 (1), 1.8654 (15), 3.3329 (50) |
| 67 | 935.365 179 | 0.0058 (1), 1.8651 (15), 3.3467 (51) |
| 68 [a] | 959.339 045 | 0.0042 (1), 1.9054 (16), 3.3762 (51) |
| 69 | 983.554 345 | 0.0013 (1), 1.9058 (16), 3.3896 (52) |
| 70 | 1008.026 399 | 0.0029 (1), 1.9049 (16), 3.4031 (53) |
| 71 [a] | 1032.736 152 | 0.0105 (1), 1.9047 (16), 3.4164 (54) |
| 72 | 1057.691 659 | 0.0074 (1), 1.9432 (17), 3.4449 (54) |
| 73 [a] | 1082.885 507 | 0.0060 (1), 1.9431 (17), 3.4578 (55) |
| 74 [a] | 1108.317 404 | 0.0111 (1), 1.9431 (17), 3.4706 (56) |
| 75 | 1133.984 273 | 0.0069 (1), 1.9802 (18), 3.4981 (56) |
| 76 [a] | 1159.893 009 | 0.0000 (1), 1.9799 (18), 3.5108 (57) |
| 77 | 1186.046 433 | 0.0041 (1), 1.9799 (18), 3.5233 (58) |
| 78 [a] | 1212.429 671 | 0.0058 (1), 1.9799 (18), 3.5357 (59) |
| 79 [a] | 1239.048 425 | 0.0062 (1), 1.9792 (18), 3.5481 (60) |
| 80 [a,b] | 1265.900 903 | 0.0039 (1), 2.0161 (19), 3.5743 (60) |
| 81 | 1292.969 098 | 0.0080 (1), 2.0500 (20), 3.6004 (60) |
| 82 | 1320.289 435 | 0.0063 (1), 2.0505 (20), 3.6123 (61) |
| 83 | 1347.835 437 | 0.6863 (2), 2.1275 (20), 3.6368 (61) |
| 84 [a] | 1375.603 457 | 0.6837 (2), 2.1595 (21), 3.6618 (61) |
| 85 | 1403.593 613 | 0.6832 (2), 2.1589 (21), 3.6735 (62) |
| 86 [a] | 1431.820 296 | 0.6807 (2), 2.1592 (21), 3.6849 (63) |
| 87 | 1460.268 068 | 0.6786 (2), 2.1898 (22), 3.7094 (63) |
| 88 | 1488.947 280 | 0.6785 (2), 2.1895 (22), 3.7208 (64) |
| 89 | 1517.853 719 | 0.6772 (2), 2.1894 (22), 3.7320 (65) |
| 90 | 1546.982 911 | 0.6751 (2), 2.1893 (22), 3.7431 (66) |
| 91 | 1576.335 999 | 0.8883 (3), 2.2573 (22), 3.7660 (66) |
| 92 [a] | 1605.905 260 | 0.8885 (3), 2.2566 (22), 3.7771 (67) |
| 93 | 1635.683 871 | 0.8843 (3), 2.3134 (24), 3.8125 (66) |
| 94 | 1665.683 010 | 0.8821 (3), 2.3127 (24), 3.8234 (67) |
| 95 | 1695.922 479 | 1.0192 (4), 2.3748 (24), 3.8455 (67) |
| 96 | 1726.376 412 | 1.0185 (4), 2.3745 (24), 3.8561 (68) |
| 97 | 1757.044 316 | 1.0198 (4), 2.3748 (24), 3.8663 (69) |
| 98 | 1787.927 516 | 1.0182 (4), 2.4008 (25), 3.8886 (69) |
| 99 | 1819.023 535 | 1.0169 (4), 2.4009 (25), 3.8988 (70) |
| 100 [a,b] | 1850.334 931 | 1.0149 (4), 2.4265 (26), 3.9205 (70) |

[a]Global minimum not found by simulated annealing. No annealing results are available in the range $N = 94–99$.

[b]Lowest-energy equilibrium improves on the minimum found by Hasse and Avilov [3].

[c]Lowest-energy equilibrium improves on the minimum found by Rafac *et al.* [2].

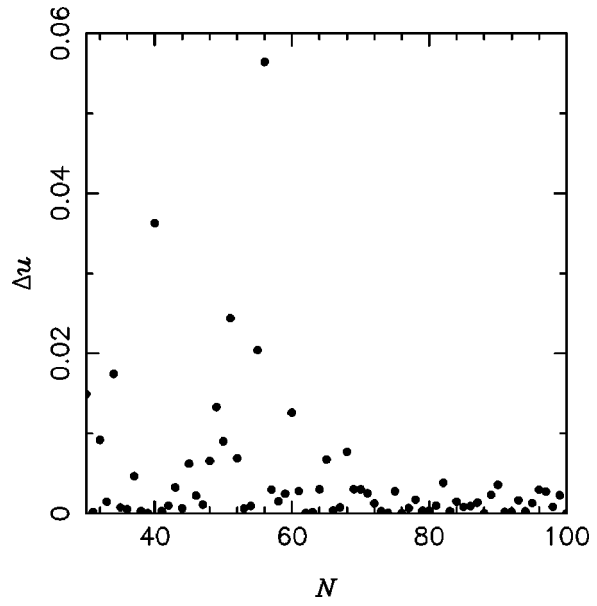


FIG. 3. Energy gaps ($\Delta u$) between the lowest and next-lowest energy configurations for $N=30$–$100$. Note the very large gap for $N=56$.

times the size of the sum of the $r^{-12}$ terms at equilibrium. Relations such as these are useful for verifying the accuracy of equilibrium structure calculations since they are very sensitive to the particle positions. Balancing conditions may prove particularly useful for verifying results obtained by methods which do not refine the solution very much, such as our simple downhill optimizer, Monte Carlo optimizers (including simulated annealers) and methods based on molecular dynamics.

It has recently been suggested by Altschuler and coworkers that the Thomson problem would make an excellent system for benchmarking optimization software [30]. Cluster problems, in general, are excellent test problems for optimizers because they are easy to code representatives of the class of NP-hard problems [31]. We suggest that the trapped ion problem studied here would make a very good test problem for techniques of unconstrained optimization. The range $N=49$–$100$ contains many cases in which the global minimum is difficult to locate, as can be seen in Table VI. Incidentally, it seems to us that the Thomson problem, suitably framed, may be an excellent test problem for optimization with constraints: Using polar coordinates, the Thomson problem is an unconstrained optimization problem in $2N-3$ coordinates [32]. However, in Cartesian coordinates, it becomes a problem with a set of nontrivial constraints.

In the protein folding problem, another notoriously hard optimization problem, lattice models suggest that proteins which fold to their native states without assistance must have a relatively large gap between the energies of the native and denatured states [33]. Figure 3 shows the energy gaps between the two configurations of lowest energy for values of $N$ between 30 and 100. At large values of $N$, these gaps tend to be small because of the large number of minima. However, there are many cases with large gaps for $N$ between 50 and 60 and a few more with moderate energy gaps for $N<70$ so that this range might be useful for testing strategies intended to be used in the protein folding problem. At larger values of $N$, relatively large gaps in the energy spectrum can still be found separating sets of minima. For instance, for $N=94$, we have found fifteen closely structurally related (67,24,3) minima within 0.0083 energy units of the lowest-energy cluster. The sixteenth minimum lies 0.0182 units above the fifteenth. This kind of energy spectrum may be generally typical of the protein energy minimization problem where there may be a few conformational substates differing by minor movements of amino-acid side chains corresponding to one overall fold.

We particularly recommend trapped-ion clusters in the $N=24$–$27$ range for dynamical study. These clusters are relatively small so that calculations in this size range are inexpensive, but they display many of the complexities of larger clusters. In particular, note from Table IV that equilibria in this range frequently occur in pairs or triplets with similar shell structures and very similar energies. One can anticipate that these minima will be separated by relatively low barriers since one can imagine paths in which one rotates the shells relative to one another without bringing ions in the two shells significantly closer to each other, especially if one allows small movements of the ions within a shell during the rotation. It would be very interesting to find out whether the temperature at which this kind of transformation between related structures becomes facile is higher or lower than the temperature at which the motion of ions within a shell displays fluid behavior [17]. In two dimensions, the barrier to rotation tends to be quite low, at least for small clusters in which the number of ions in the inner shell is not an integral multiple of the number of outer-shell ions [29].

## ACKNOWLEDGMENTS

We would like to thank the Department of Mathematics and Computer Science at the University of Lethbridge for access to their network of Sun workstations. M.R.R. is grateful to Keramat Ali for useful discussions. This work was funded by a grant from the Natural Sciences and Engineering Research Council of Canada to M.R.R. In addition, R.A.B. was supported by the University of Lethbridge.

[1] D. J. Wineland, J. C. Bergquist, W. M. Itano, J. J. Bollinger, and C. H. Manney, Phys. Rev. Lett. **59**, 2935 (1987).
[2] R. Rafac, J. P. Schiffer, J. S. Hangst, D. H. E. Dubin, and D. J. Wales, Proc. Natl. Acad. Sci. USA **88**, 483 (1991).
[3] R. W. Hasse and V. V. Avilov, Phys. Rev. A **44**, 4506 (1991).
[4] E. L. Alschuler, T. J. Williams, E. R. Ratner, F. Dowla, and F. Wooten, Phys. Rev. Lett. **72**, 2671 (1994).
[5] T. Erber and G. M. Hockney, Phys. Rev. Lett. **74**, 1482 (1995).
[6] E. L. Altschuler, T. J. Williams, E. R. Ratner, F. Dowla, and F. Wooten, Phys. Rev. Lett. **74**, 1483 (1995).
[7] D. J. Wales and A. M. Lee, Phys. Rev. A **47**, 380 (1993).
[8] D. H. E. Dubin, Phys. Rev. Lett. **71**, 2753 (1993).

[9] J. P. Schiffer, Phys. Rev. Lett. **70**, 818 (1993).
[10] M. R. Hoare and J. A. McInnes, Adv. Phys. **32**, 791 (1983).
[11] Yu. E. Lozovik and V. A. Mandelshtam, Phys. Lett. A **145**, 269 (1990).
[12] A. Corana, M. Marchesi, C. Martini, and S. Ridella, ACM Trans. Math. Softw. **13**, 262 (1987).
[13] D. J. Wales and J. P. K. Doye, J. Phys. Chem. A **101**, 5111 (1997).
[14] J. Mostowski and M. Gajda, Acta Phys. Pol. A **67**, 783 (1985).
[15] E. V. Baklanov and V. P. Chebotayev, Appl. Phys. B: Photophys. Laser Chem. **39**, 179 (1986).
[16] J. Uppenbrink and D. J. Wales, Chem. Phys. Lett. **190**, 447 (1992).
[17] D. H. E. Dubin and T. M. O'Neil, Phys. Rev. Lett. **60**, 511 (1988).
[18] K. Tsuruta and S. Ichimaru, Phys. Rev. A **48**, 1339 (1993).
[19] J. R. Edmundson, Acta Crystallogr., Sect. A: Found. Crystallogr. **48**, 60 (1992).
[20] A. A. Berezin, Phys. Scr. **43**, 111 (1991).
[21] F. A. Cotton and G. Wilkinson, in *Advanced Inorganic Chemistry*, 4th ed. (Wiley, New York, 1980), pp. 196 and 197.
[22] V. M. Bedanov and F. M. Peeters, Phys. Rev. B **49**, 2667 (1994).
[23] R. W. Hasse, Acta Phys. Pol. B **25**, 589 (1994).
[24] A. Rahman and J. P. Schiffer, Phys. Rev. Lett. **57**, 1133 (1986).
[25] H. Totsuji and J.-L. Barrat, Phys. Rev. Lett. **60**, 2484 (1988).
[26] J. P. Schiffer, Phys. Rev. Lett. **61**, 1843 (1988).
[27] S. L. Gilbert, J. J. Bollinger, and D. J. Wineland, Phys. Rev. Lett. **60**, 2022 (1988).
[28] G. Birkl, S. Kassner, and H. Walther, Nature (London) **357**, 310 (1992).
[29] V. A. Schweigert and F. M. Peeters, Phys. Rev. B **51**, 7700 (1995).
[30] E. L. Altschuler, T. J. Williams, E. R. Ratner, R. Tipton, R. Stong, F. Dowla, and F. Wooten, Phys. Rev. Lett. **78**, 2681 (1997).
[31] L. T. Wille and J. Vennik, J. Phys. A **18**, L419 (1985).
[32] T. W. Melnyk, O. Knop, and W. R. Smith, Can. J. Chem. **55**, 1745 (1977).
[33] A. Šali, E. Shakhnovich, and M. Karplus, J. Mol. Biol. **235**, 1614 (1994).
[34] Coordinate files for all equilibria and saddle points found in this study are available by email to roussel@uleth.ca